Bulletin of Electrical Engineering and Informatics
Vol. 12, No. 5, October 2023, pp. 2801~2806
ISSN: 2302-9285, DOI: 10.11591/eei.v12i5.5344

Spatial uniformity of the spectral radiance by white LED-based $K_2CaP_2O_7:Ce^{3+}$, Tb^{3+} phosphor

Ha Thanh Tung[1], My Hanh Nguyen Thi[2]
[1]Faculty of Basic Sciences, Vinh Long University of Technology Education, Vinh Long, Vietnam
[2]Faculty of Mechanical Engineering, Industrial University of Ho Chi Minh City, Ho Chi Minh City, Vietnam

Article Info

Article history:

Received Nov 27, 2022
Revised Dec 16, 2022
Accepted Jan 11, 2023

Keywords:

$K_2CaP_2O_7:Ce^{3+}$, Tb^{3+}
Light-emitting diodes devices
Luminescent
Phosphors
Spectrum

ABSTRACT

The $K_2CaP_2O_7:Ce^{3+}$, Tb^{3+} (Ce/Tb-KCPO) phosphor with blue-to-green emission is introduced in this study. The synthesis of the phosphor is carried out with the solid-state approach. The phosphor characteristics, including X-ray diffraction, luminescence lifespan, and thermal stability are measured and examined. The data show that Ce/Tb-KCPO phosphor displays a broadband emission from blue to green when excited by ultraviolet source. Besides, the ion Ce^{3+} strengthen the emission of Tb^{3+} ion through an efficient energy-transfer mechanism, which is estimated about 82.51%. The main electric interaction responsible for this Ce/Tb energy transfer is the dipole-quadrupole one. The phosphor also benefits the luminous intensity and color uniformity of the light-emitting diodes (LED) white-light output. Therefore, the Ce/Tb-KCPO phosphor can be a potential material for high-power white light-emitting diodes (WLED).

Corresponding Author:

My Hanh Nguyen Thi
Faculty of Mechanical Engineering, Industrial University of Ho Chi Minh City
No. 12 Nguyen Van Bao Street, Ho Chi Minh City, Vietnam
Email: nguyenthimyhanh@iuh.edu.vn

1. INTRODUCTION

With exceptional properties like great brightness, long-term service, ease of manufacture, and low toxicity, inorganic luminescence compounds have been the topic of many researchers' interest [1], [2]. One of the most promising materials is the rare-earth-based compounds [3]. The rare earth ions have a unique 4F shell arrangement, allowing them to be able to produce good hues. By mixing various rare earth ions and adjusting the ion dopant's ratio, it is possible to obtain distinguish excitation energies and nearly the whole visible light spectrum from violet to red. In terms of green spectral wavelength, the ion Tb^{3+} is a typical activator for its strong emission centered at roughly 545 nm, owing to the transition of $^5D_4 \rightarrow {}^7F_5$ [4]–[6]. Nevertheless, using only Tb^{3+} ion in a phosphor host is insufficient for practical uses owing to its inferior absorption lines of 4F-4F spin-forbidden transitions [7]. However, the emission strength of Tb^{3+} can be heightened using a suitable sensitizer, especially Ce^{3+} ions. Meanwhile, depending on the nature of the base materials, the co-doped phosphor typically shows an absorption band of f-d for Ce^{3+}, which extends from ultraviolet to visible light, making it possible to greatly widen Tb^{3+} applications [8].

The host lattice for doping Ce^{3+} and Tb^{3+} also has an imperative effect on the phosphor material's performance. Among the host materials, pyrophosphate has been demonstrated a broadband gap and high-efficiency material, which also offers excellent thermal and chemical stability [9], [10]. It was reported that the phosphor with pyrophosphate host could be synthesized at a lower heat (not exceeding 800 ^oC) than other base such as aluminates or silicates (>1,200 ^oC). In the pyrophosphate variations, $K_2CaP_2O_7$ (KCPO) contains enough substitutable space for the rare earth ions. Given the benefits listed above, KCPO could be an excellent host lattice for luminous compounds. However, there has been limited study on KCPO hosts and on Ce^{3+}/Tb^{3+}-co-activated KCPO material [11], [12].

In this research, we center on the development of a KCPO-based phosphor with small amount of energy consumption and great thermal stability. In addition, the investigation of the luminous performance of Ce^{3+} and Tb^{3+} in the KCPO host is also demonstrated. The phosphor was produced using the solid-state technique. To validate the phosphors' purity and the influence of the dopants' amount on crystal geometry, the crystal phase and site replacement were explored. To understand the luminous mechanism of the ion dopants as well as the power shift process among Ce^{3+} and Tb^{3+} within the KCPO base, the luminous performance including excitation, emission spectra, along with the chromaticity diagram was reviewed. Furthermore, thermal stability was investigated in order to investigate potential effectiveness.

2. METHOD

2.1. Creating $K_2CaP_2O_7$:Ce^{3+}, Tb^{3+} (Ce/Tb-KCPO)

The phosphor with blue-green phosphor Ce/Tb-KCPO was synthesized utilizing the solid-state technique. The chemical elements of the phosphor composition and synthesizing process of the phosphor were presented in Table 1 [13]. The employed elements are uncomtaminated.

Table 1. Raw ingredients and synthesizing process of Ce/Tb-KCPO phosphor

Materials	Purity (%)	Synthesizing procedure
K_2CO_3	99.99	1. The uncomtaminated ingredients were weighed stoichiometrically and well mixed in a mortar.
$CaCO_3$	99.99	2. The mixture was ground thoroughly.
$NH_4H_2PO_4$	99.99	3. The ground sample was calcined in an alumina crucible at ~780 ºC for four hours, with 5 vol
CeO_2	99.99	% H_2 in N_2.
Tb_4O_7	99.99	4. The phosphor sample was cooled down to room temperature and re-ground.

2.2. Phosphor characteristics and measuring instruments

Table 2 shows the characteristics of the prepared phosphor that were examined and the corresponding determing instruments [14]. Besides, the phosphor was applied to create a white light-emitting diodes (WLED) model for further investigations. Figure 1 shows the components and the structure of the required WLED package. Figure 1(a) is the true photograph of the WLED model; Figures 1(b) and (c) display the diagram of bonding light-emitting diodes (LED) chip and the phosphor-layer organization in the model; Figure 1(d) shows the WLED 3D simulation built by the LightTools software [15], [16]. Here, the influences of the Ce/Tb-KCPO is examined with the variation of its concentration (wt %), and the results will be discussed in the next section.

Table 2. Characteristics of the phosphor and corresponding measuring instruments

Characteristics	Instruments
Patterns of X-ray diffraction (XRD)	Bruker D8 advance, with 2θ range of 10-60º, a radiation Cu-Kα (~0.15405 nm), at 30 kV and 40 mA.
Emission spectrum and excitation spectrum	Hitachi F-4500 fluorescence spectrophotometer, with excitation source of a Xe lamp (150 W).
Luminescent lifetime and thermal stability	HORIBA Jobin Yvon Fluorolog-3.

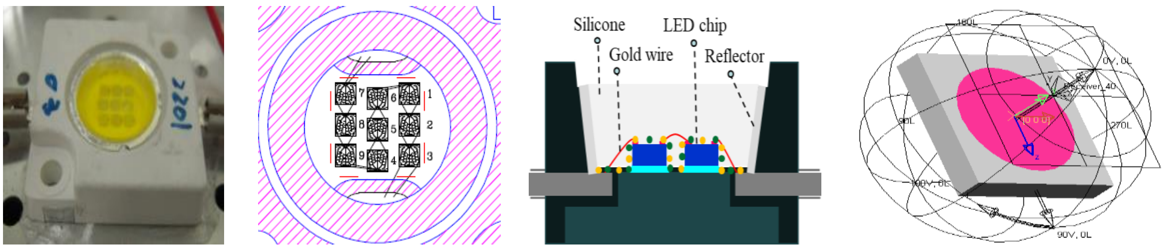

(a) (b) (c) (d)

Figure 1. Pictures depicting WLED formation (a) WLED device, (b) binding graph, (c) pc-WLED illustrated, and (d) recreating WLED device via program LightTools

3. RESULTS AND DISCUSSION

3.1. Computation

The energy transfer process of the doped ions in the host can affect the emission performance of the phosphor. This feature of the Ce/Tb-KCPO phosphor can be mathematically determined by estimating the critical distance Rc among the ions of Tb^{3+} and Ce^{3+}. The Rc could be determined through the expression of concentration quenching in (1) [17]:

$$Rc \approx 2 \times [(3V)/(4\pi XcN)]^{1/3} \quad (1)$$

Where V, Xc, and N represent the unit-cell volume, the sum optimal concentration of Tb^{3+} and Ce^{3+}, and the center cation's number in the crystal, respectively. For the KCPO host, we get the values of V, Xc, and N of 700.94 $Å^3$, 0.14, and 4, respectively. As a result, the obtained Rc is about 13.37 Å, which greatly exceeds 5 Å. Therefore, the Ce^{3+}/Tb^{3} ion power shift process in the host would be attributed to the electric multipolar interaction. Then, the multipolar-interaction kind can be determined with Dexter-theory in (2):

$$\frac{\eta_0}{\eta} \infty C^{n/3} \quad (2)$$

Where n can be 6, 8, and 10. With n=6, the interaction is dipole-dipole, while n=8 is dipole-quadrupole and n=10 is quadrupole-quadrupole. η and η_0 represent the Ce^{3+} luminous quantum efficacy in the Tb^{3+} presence and absence, respectively. C indicates the activators' concentration. Based on the approximation of Reisfeld, $\frac{\eta_0}{\eta}$ can be altered by the related-luminescence intensities' ratio ($\frac{I_{SO}}{I_S}$), as expressed in (3) [18]:

$$\frac{I_{SO}}{I_S} \infty C^{n/3} \quad (3)$$

Where I_{SO} is the luminescent strength of the KCPO:xCe^{3+} (x=0.02), and I_S is the luminescent strength of xCe/yTb-KCPO (x=0.02; y=0–0.2). In regard to the $\frac{I_{SO}}{I_S}$ dependence on $C^{6/3}$, $C^{8/3}$, and $C^{10/3}$ for Ce^{3+} emission, the linear connection could be recorded as n=8, which means the dipole-quadrupole interactivity would be the most significant for the Ce^{3+}/Tb^{3+} power shift within the KPCO base. The temperature-dependent luminescent strength (S_T) and the activation power (P_a) can be clarified and using (4) [19]:

$$S_T = \frac{S_0}{1 + c\ exp[P_a/(-kT)]} \quad (4)$$

where S_T and S_0 represent the luminescent strength of Tb^{3+} at the temperatures of different measurements and at room temperature, respectively, c signifies a constant, k signifies Boltzmann constant.

3.2. Phosphor influence on white light-emitting diodes

When the phosphor Ce/Tb-KCPO is used in the WLED model, the concentration of the phosphor has significant effects on the lighting properties of the WLED. The scattering of the forward scattering of the light seems to be enhanced with the presence of this blue-green emission phosphor. Figure 2 displays the reduced scattering coefficients (RSC) of the WLED with increasing concentration of Ce/Tb-KCPo phosphor. The figure presents that the increasing phosphor concentration leads to the increase in the RSC, meaning that the backward scattering is possibly reduces, allowing more light to transmit through the phosphor layer and escape from the LED [20]. As a result, the light output intensity can be enhanced.

Besides, the addition of Ce/Tb-KCPO cause the YAG:Ce yellow-phosphor concentration to decreases to serve the purpose of stabilizing correlated color temperature (CCT). This phenomenon is displayed by Figure 3. The higher the concentration for Ce/Tb-KCPO, the lower the YAG:Ce concentration. Moreover, the decrease of YAG:Ce content helps increase the forward scattering and enhance the color uniformity of the generated white light.

Figures 4 and 5 help clarify the benefits of Ce/Tb-KCPO improving the hue uniformity for the WLED light output. Particularly, Figure 4 shows the CCT values for the WLED with different concentration of Ce/Tb-KCPO, while Figure 5 shows the decline in CCT deviation (D-CCT, color deviation) [21]. Obviously, the increasing of the blue-green phosphor (0–25%) can keep the variation of CCT to the lower level. 25% Ce/Tb-KCPO shows the lowest CCT deviation (Figure 5), indicating that the color uniformity with 25% concentration of this phosphor is the highest.

Besides the color uniformity, the color rendition ability of the white-light is important. The rendition ability of the white light with increasing concentration of Ce/Tb-KCPO phosphor can be validated via the color rendering index (CRI) along with color quality scale (CQS), which will be shown in Figures 6 and 7, respectively. As illustrated, heightened concentration values of the phosphor decrease the CRI and CQS [22]–[24]. The color rendition can be enhanced with wide-band emission that can cover the orange-red region. However, the emission of the Ce/Tb-KCPO is strong between the blue and green regions and weak in the orange-red band. Consequently, the red component is not enough to give good combination for the improved CRI and CQS. Additionally, the strong absorption of the Ce/Tb-KCPO is partially attributed to the declining CQS and CRI. Particularly, the phosphor granules strongly absorbed the blue illumination generated by LED chip as well as the yellow illumination generated by the phosphor YAG:Ce, which allows the phosphor to convert these lights to generate more green lights. Hence, the green light components are much greater than the others, making the light inefficiently rendering the color as expected.

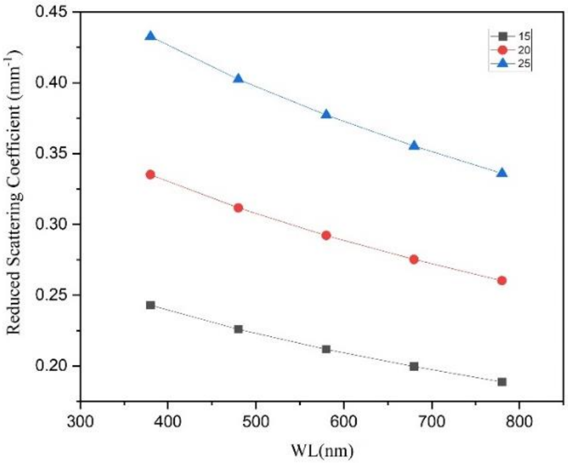

Figure 2. RSC with increasing Ce/Tb-KCPO content

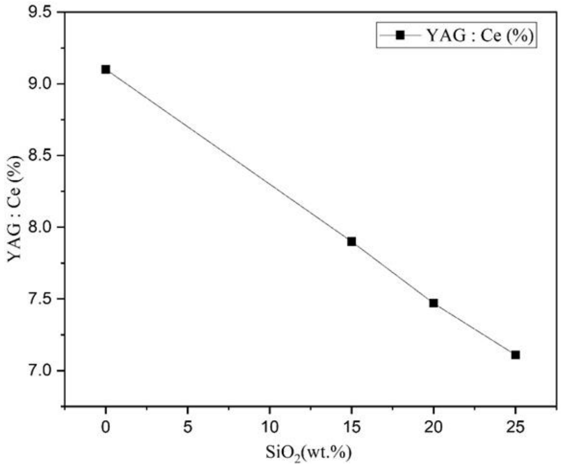

Figure 3. YAG:Ce weight percentage reducing with increasing Ce/Tb-KCPO concentration

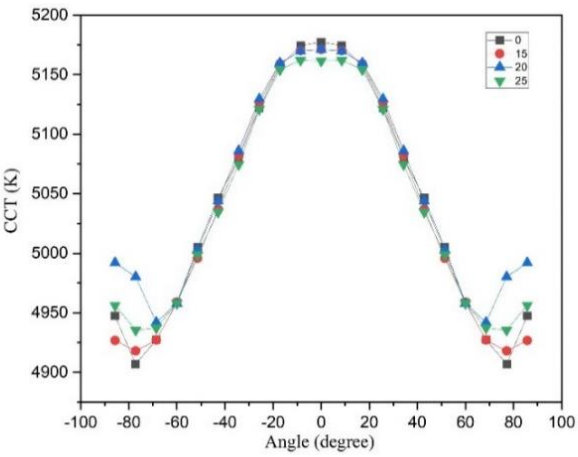

Figure 4. WLED's CCT values change with the concentration of the Ce/Tb-KCPO phosphor

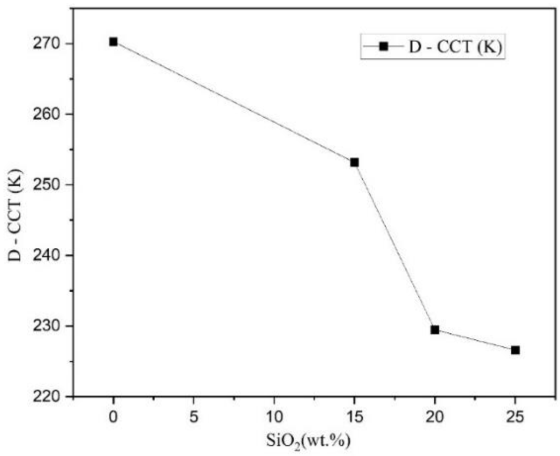

Figure 5. WLED's CCT deviation along with Ce/Tb-KCPO concentration

The luminous of the WLED with Ce/Tb-KCPO is also a critical category to assess. Figure 8 shows the rise in luminosity of the WLED if the concentration for the Ce/Tb-KCPO phosphor increase from 0% to 25%. This means the total light escaping from the LED dome is enhanced. It is possibly ascribed to the enhanced forward scattering and stronger blue-green emission. Figure 9 displays the total emission power of the WLED with Ce/Tb-KCPO phosphor (0–25%), from which the stimulated blue-green emission regions can be clarified. The figure depicts the two peaks of the WLED emission in the blue region at ~450 nm and green region at ~545 nm. So, the Ce/Tb-KCPO phosphor can be useful in obtaining greater luminosity along with enhanced color uniformity for WLED light [25].

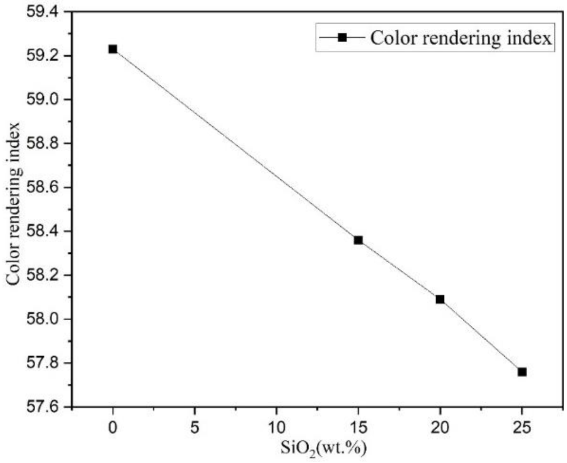

Figure 6. WLED's color rendering index with different Ce/Tb-KCPO concentrations

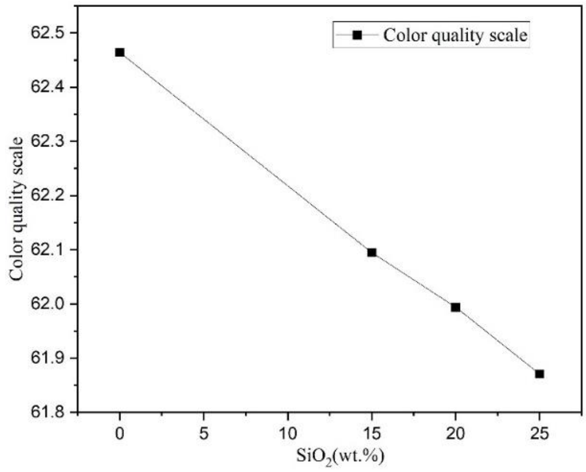

Figure 7. WLED's color quality scale with Ce/Tb-KCPO phosphor presence

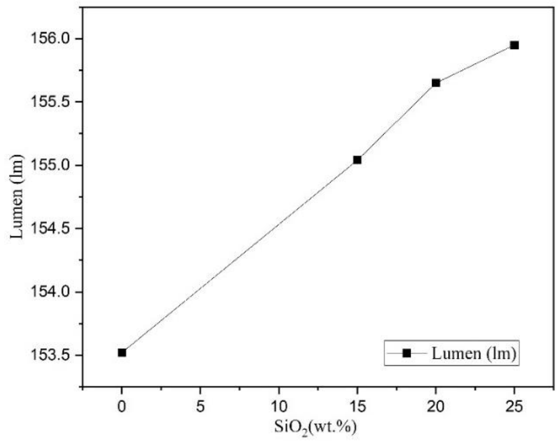

Figure 8. WLED's lumen with different Ce/Tb-KCPO concentrations

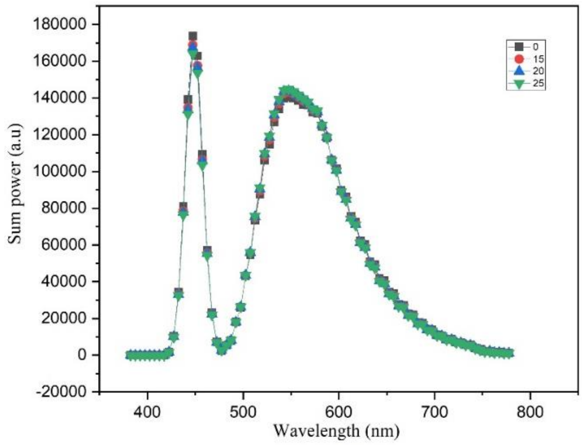

Figure 9. WLED's emission power with Ce/Tb-KCPO phosphor presence

4. CONCLUSION

This study demonstrated the Ce/Tb-KCPO phosphor with blue-green emission, which can be prepared using solid-state synthesizing method. The optimal luminescence of the phosphor can be obtained by modifying the concentration of the ion dopants. The phosphor shows blue-green emission color as a result of the energy-transferring influence of $Ce^{3+} \rightarrow Tb^{3+}$. The energy transfer strength varies with the increasing content of the Tb^{3+} ion dopant in the phosphor composition. The electric interaction of dipole-quadrupole is observed to be responsible for the power shift process among the activated ions within the KCPO host. Besides, the phosphor exhibits good thermal stability with the temperature range of 77–673 K. The phosphor also demonstrates its advantage in stimulating the luminescent intensity and uniform color properties of the white light from the as-prepared WLED model. The color rendition performance, on the other hand, steadily decreases as the phosphor content increase, according to the decline of both CRI and CQS values. Thus, the Ce/Tb-KCPO phosphor have potential in solid-state lighting technology and high-power LED devices.

REFERENCES

[1] Z. Zhang and W. Yang, "Tunable photoluminescence in Ba 1-x SrxSi 3 O 4 N 2 : Eu 2+ / Ce 3+ , Li + solid solution phosphors induced by linear structural evolution," *Optical Materials Express*, vol. 9, no. 4, pp. 1922–1932, Apr. 2019, doi: 10.1364/OME.9.001922.

[2] S. K. Abeysekera, V. Kalavally, M. Ooi, and Y. C. Kuang, "Impact of circadian tuning on the illuminance and color uniformity of a multichannel luminaire with spatially optimized LED placement," *Optics Express*, vol. 28, no. 1, pp. 130–145, 2020, doi: 10.1364/OE.381115.

[3] A. Ali *et al.*, "Blue-laser-diode–based high CRI lighting and high-speed visible light communication using narrowband green-/red-emitting composite phosphor film," *Applied Optics*, vol. 59, no. 17, pp. 5197–5204, Jun. 2020, doi: 10.1364/ao.392340.

[4] Y. Tang, Z. Li, G. Liang, Z. Li, J. Li, and B. Yu, "Enhancement of luminous efficacy for LED lamps by introducing polyacrylonitrile electrospinning nanofiber film," *Optics Express*, vol. 26, no. 21, pp. 27716–27725, Oct. 2018, doi: 10.1364/OE.26.027716.

[5] X. Ding *et al.*, "Improving the optical performance of multi-chip LEDs by using patterned phosphor configurations," *Optics Express*, vol. 26, no. 6, pp. 283–292, Mar. 2018, doi: 10.1364/OE.26.00A283.

[6] M. J. Egan, A. Colón, S. M. Angel, and S. Sharma, "Suppressing the multiplex disadvantage in photon-noise limited interferometry using cross-dispersed spatial heterodyne spectrometry," *Applied Spectroscopy*, vol. 75, no. 2, pp. 208–215, 2020, doi: 10.1177/0003702820946739.

[7] H. Daicho, K. Enomoto, H. Sawa, S. Matsuishi, and H. Hosono, "Improved color uniformity in white light-emitting diodes using newly developed phosphors," *Optics Express*, vol. 26, no. 19, pp. 24784–24791, Sep. 2018, doi: 10.1364/OE.26.024784.

[8] N. C. Abd Rashid *et al.*, "Spectrophotometer with enhanced sensitivity for uric acid detection," *Chinese Optics Letters*, vol. 17, no. 8, pp. 1–5, 2019, doi: 10.3788/COL201917.081701.

[9] M. J. H. Anthonissen, L. B. Romijn, J. H. M. T. T. Boonkkamp, and W. L. IJzerman, "Unified mathematical framework for a class of fundamental freeform optical systems," *Optics Express*, vol. 29, no. 20, pp. 31650–31664, Sep. 2021, doi: 10.1364/OE.438920.

[10] A. A. Pan'kov, "Informative light pulses of indicating polymer fiber-optic piezoelectroluminescent coatings upon indentation of rigid globular particles," *Journal of Optical Technology*, vol. 88, no. 8, pp. 477–482, Aug. 2021, doi: 10.1364/JOT.88.000477.

[11] J. X. Yang, D. S. Li, G. Li, E. Y. B. Pun, and H. Lin, "Photon quantification in Ho 3+ /Yb 3+ co-doped opto-thermal sensitive fluotellurite glass phosphor," *Applied Optics*, vol. 59, no. 19, pp. 5752–5763, Jul. 2020, doi: 10.1364/AO.396393.

[12] J. Hao, H.-L. Ke, L. Jing, Q. Sun, and R.-T. Sun, "Prediction of lifetime by lumen degradation and color shift for LED lamps, in a non-accelerated reliability test over 20,000 h," *Applied Optics*, vol. 58, no. 7, pp. 1855–1861, Mar. 2019, doi: 10.1364/AO.58.001855.

[13] A. K. Dubey, M. Gupta, V. Kumar, and D. S. Mehta, "Laser-line-driven phosphor-converted extended white light source with uniform illumination," *Applied Optics*, vol. 58, no. 9, pp. 2402–2407, Mar. 2019, doi: 10.1364/AO.58.002402.

[14] Z. Zhuang, D. Iida, P. Kirilenko, M. Velazquez-Rizo, and K. Ohkawa, "Optimal ITO transparent conductive layers for InGaN-based amber/red light-emitting diodes," *Optics Express*, vol. 28, no. 8, pp. 12311–12321, Apr. 2020, doi: 10.1364/OE.389725.

[15] Y. Cheng and K. Sun, "Color modification of ZnGa 2 O 4 :Yb 3+ ,Er 3+ ,Tm 3+ upconversion phosphors with the doping of Sn 4+ and Ge 4+ ions," *Applied Optics*, vol. 59, no. 24, pp. 7313–7320, Aug. 2020, doi: 10.1364/AO.399519.

[16] L. Xie *et al.*, "Highly luminescent and stable lead-free cesium copper halide perovskite powders for UV-pumped phosphor-converted light-emitting diodes," *Photonics Research*, vol. 8, no. 6, pp. 768–775, Jun. 2020, doi: 10.1364/PRJ.387707.

[17] S. P. Groth, A. G. Polimeridis, A. Tambova, and J. K. White, "Circulant preconditioning in the volume integral equation method for silicon photonics," *Journal of the Optical Society of America A*, vol. 36, no. 6, pp. 1079–1088, Jun. 2019, doi: 10.1364/JOSAA.36.001079.

[18] M. Quesada *et al.*, "All-glass, lenticular lens light guide plate by mask and etch," *Optical Materials Express*, vol. 9, no. 3, pp. 1180–1190, Mar. 2019, doi: 10.1364/OME.9.001180.

[19] S. Rasouli, S. Hamzeloui, and D. Hebri, "Colorful radial Talbot carpet at the transverse plane," *Optics Express*, vol. 27, no. 13, pp. 17435–17448, Jun. 2019, doi: 10.1364/OE.27.017435.

[20] X. Liu *et al.*, "Upconversion luminescence, intrinsic optical bistability, and optical thermometry in Ho3+/Yb3+: BaMoO4 phosphors," *Chinese Optics Letters*, vol. 17, no. 11, pp. 1–4, 2019, doi: 10.3788/COL201917.111601.

[21] M. Lange, N. Kiss, L. Fesus, E. V. Plorina, A. Derjabo, and J. Spigulis, "Non-invasive LED-based screening solution for skin cancer," in *Clinical and Preclinical Optical Diagnostics II*, Jul. 2019, pp. 1–5, doi: 10.1117/12.2526386.

[22] M. Dupont-Nivet, C. I. Westbrook, and S. Schwartz, "The role of trap symmetry in an atom-chip interferometer above the bose-Einstein condensation threshold," in *2019 Conference on Lasers and Electro-Optics Europe & European Quantum Electronics Conference (CLEO/Europe-EQEC)*, Jun. 2019, pp. 1–3, doi: 10.1109/CLEOE-EQEC.2019.8872823.

[23] C. Zheng, H. Zhu, Z. Xu, R. K. Sinha, Q. Li, and P. Ghosh, "High-efficient photoacoustic generation with an ultrathin metallic multilayer broadband absorber," *Optics Express*, vol. 29, no. 6, pp. 8490–8497, Mar. 2021, doi: 10.1364/OE.420138.

[24] Y. Fang *et al.*, "Giant enhancement of white light emission from Ca 9 Ln(PO 4) 7 :Eu 2+ ,Mn 2+ (Ln = La, Lu, Gd) phosphors achieved by remote aluminum reduction," *Optical Materials Express*, vol. 10, no. 5, pp. 1306–1322, May 2020, doi: 10.1364/OME.390069.

[25] D. T. Tuyet *et al.*, "Deep red fluoride dots-in-nanoparticles for high color quality micro white light-emitting diodes," *Optics Express*, vol. 28, no. 18, pp. 26189–26199, Aug. 2020, doi: 10.1364/OE.400848.

BIOGRAPHIES OF AUTHORS

Ha Thanh Tung received the PhD degree in physics from University of Science, Vietnam National University Ho Chi Minh City, Vietnam, he is working as a lecturer at the Faculty of Basic Sciences, Vinh Long University of Technology Education, Vietnam. His research interests focus on developing the patterned substrate with micro-and nano-scale to apply for physical and chemical devices such as solar cells, OLED, photoanode. He can be contacted at email: tunght@vlute.edu.vn.

My Hanh Nguyen Thi received a Bachelor of Physics from An Giang University, VietNam, Master of Theoretical Physics and Mathematical Physics, Hanoi National University of Education, VietNam. Currently, she is a lecturer at the Faculty of Mechanical Engineering, Industrial University of Ho Chi Minh City, Viet Nam. Her research interests are theoretical physics and mathematical physics. She can be contacted at email: nguyenthimyhanh@iuh.edu.vn.